Maximum likelihood estimation of direction of arrival using an acoustic vector-sensor

Dovid Levin
Faculty of Engineering, Bar-Ilan University, Ramat-Gan, Israel

Emanuël A. P. Habets[a)]
International Audio Laboratories Erlangen,[b)] Erlangen, Germany

Sharon Gannot
Faculty of Engineering, Bar-Ilan University, Ramat-Gan, Israel

(Received 13 July 2011; revised 20 December 2011; accepted 22 December 2011)

A vector-sensor consisting of a monopole sensor collocated with orthogonally oriented dipole sensors is used for direction of arrival (DOA) estimation in the presence of an isotropic noise-field or internal device noise. A maximum likelihood (ML) DOA estimator is derived and subsequently shown to be a special case of DOA estimation by means of a search for the direction of maximum steered response power (SRP). The problem of SRP maximization with respect to a vector-sensor can be solved with a computationally inexpensive algorithm. The ML estimator achieves asymptotic efficiency and thus outperforms existing estimators with respect to the mean square angular error (MSAE) measure. The beampattern associated with the ML estimator is shown to be identical to that used by the minimum power distortionless response beamformer for the purpose of signal enhancement. © *2012 Acoustical Society of America*. [DOI: 10.1121/1.3676699]

PACS number(s): 43.60.Jn, 43.60.Fg [EJS] Pages: 1240–1248

I. INTRODUCTION

One of the classical problems in the realm of acoustical signal processing is direction of arrival (DOA) estimation. This is a major component of the source localization problem, which besides DOA estimation also includes range estimation. Applications of DOA estimation include such areas as surveillance, navigation, and tracking. In many specific examples, such as automated steering of cameras, knowledge of the DOA (without range) is sufficient.

Various factors such as reverberation, and noise originating from the sensors, from directional interference, or from the ambient environment often impose complications upon the estimation of DOA. The current paper is concerned with nondirectional (isotropic) noise, which may result from internal sensor noise or external diffuse noise. Estimation of DOA in reverberant environments and the resulting bias, have been investigated[1,2] in the context of an intensity-based algorithm.

Conventional approaches for DOA estimation utilize an array of pressure sensors, which have been distributed at different locations. The present paper deals with measurements obtained by an acoustical vector-sensor, which consists of four collocated sensor elements: One monopole receiver and three orthogonally oriented dipole receivers. In practical terms, the monopole is produced by an omnidirectional microphone and the dipoles are obtained from sensors measuring particle-velocity, which are appropriately scaled.[1] Vector-sensors based on microelectromechanical systems technology, which measure particle-velocity, have become available.[3] An alternative approach[4] uses measurements from closely spaced pressure sensors to approximate the *spatial derivative* of the sound-field in a given direction, which possesses dipole directivity. Incorporation of delays between sensor elements has the effect of producing a monopole component, which allows for the creation of any first-order beampattern. Combining spatial derivatives with different orientations enables steering of the beampattern.[5]

Although the approach of differential approximation does not require novel sensor devices, it is known to suffer from high white noise gain, accentuating the importance of efficient performance in the presence of noise. Furthermore, the accuracy of a spatial derivative requires that the distance between sensors be small with respect to the acoustical wavelength[6] ($d \ll \lambda$). At high frequencies this assumption fails, leading to distorted beampatterns. Hence, in the design of a differential vector-sensor the distance d must be set within an upper bound, which limits distortion at the highest frequency of interest to acceptable or negligible levels.[7] The present paper assumes a single vector-senor with ideal monopole and dipole beampatterns operating on a wideband signal and is not tied to any particular method used to obtain these beampatterns.

A brief comparison between conventional array processing and vector-sensor processing reveals several insights. A vector-sensor provides more information than a pressure sensor as it contains three dipole channels in addition to a monopole channel. Hence, an array of N vector-sensors can achieve better performance than a conventional array of N pressure sensors.[8,9] Likewise, a given level of performance may be attained with fewer vector-sensors. A conventional array requires ample spacing between multiple elements, whereas a single vector-sensor can accomplish spatial processing with a compact configuration. Furthermore, the performance of conventional

[a)]Author to whom correspondence should be addressed. Electronic mail: emanuel.habets@audiolabs-erlangen.de
[b)]A joint institution between the Friedrich-Alexander University of Erlangen-Nuremberg and Fraunhofer IIS, Germany.

 0001-4966/2012/131(2)/1240/9/$30.00

arrays is highly dependent upon signal frequency; this is not the case for a single vector-sensor (where by design $d \ll \lambda$). Due to these attractive characteristics, the use of vector-sensors for signal processing has recently garnered considerable interest.

On the other side, the performance of a single vector-sensor is somewhat limited. For example, the maximum directivity index (DI) attainable with a single vector-sensor is limited to 6 dB.[8] With a conventional array, higher DIs are attainable, although this typically requires use of additional sensors and additional space. As a single vector-sensor is subject to inherent limitations, it is important to determine the precise extent of its capabilities.

In this respect, the seminal work of Nehorai and Paldi[10] pertaining to DOA estimation with vector-sensors is particularly significant. They define the mean square angular error (MSAE) criterion for evaluating estimation performance and then compute the Cramér-Rao lower bound (CRLB) for an array of vector-sensors operating in a scenario with uncorrelated Gaussian source and noise signals. Their work led the way to further research in the realm of signal processing with vector sensors. Studies pertaining to signal-processing with a *single* vector-sensor has been conducted with respect to DOA estimation,[10–14] beamforming,[15–17] and communication.[18,19]

Nehorai and Paldi[10] proposed two different algorithms for DOA estimation with a single vector-sensor (under the names *Intensity-Based Algorithm* and *Velocity-Covariance-Based Algorithm*) and evaluated their performance by calculating the MSAEs. Neither of the algorithms achieves the CRLB. In a previous study,[20] a DOA estimation method based on a search for the direction of maximum steered response power (SRP) was proposed by the authors (similar to that of Ref. 21 in the context of conventional arrays). Algorithms mentioned in earlier works[10,22] were shown to be special cases of the proposed maximum SRP method. Furthermore, it was demonstrated that with a suitable choice of parameter one may obtain a DOA estimator, which approaches the CRLB. However, it was not clear in advance (i.e., without prior testing), which choice of parameter would be optimal.

The current study proposes a maximum likelihood (ML) estimation scheme for determining DOA with a single vector-sensor. In general, ML-DOA estimation with an array of sensors entails an unwieldy maximization problem. In the present case, it is shown that the obtained estimator is equivalent to a specific realization of the maximum SRP method. Maximization of SRP for a single vector-sensor can be performed with a computationally inexpensive algorithm.[20] Although the maximum SRP method with an *arbitrary* selection of beampattern parameter is suboptimal, the specific realization relating to ML estimation corresponds to an optimal selection of beampattern and attains the CRLB. It is further demonstrated that the minimum power distortionless response (MPDR) beamformer (from the field of signal enhancement and spectral estimation) shares the same beampattern. Thus, the complementary problems of DOA estimation, which involves *maximization* of power through beam steering, and MPDR beamforming, which involves *minimization* of power by beam shaping, meet on common ground. Both problems admit identical beampatterns to yield an optimal solution.

The remainder of this paper is organized as follows. In Sec. II, the DOA problem is described in detail and the MSAE measure of accuracy is defined. In Sec. III, the ML estimator is derived and presented in terms of the sample covariances pertaining to the different sensor elements. Section IV describes how the ML estimator relates to DOA estimation by means of a search for the direction of maximum SRP. Similarly, an affinity between the ML estimator and the MPDR beamformer is shown. In Sec. V, the performance of the ML estimator is presented in terms of MSAE and is compared with the estimators proposed in Ref. 10. Finally, Sec. VI concludes with a brief summary.

II. PROBLEM FORMULATION AND PRELIMINARIES

A signal propagates through space from a source toward a receiver in an anechoic environment. Our objective is to determine its DOA, which is represented by the unit vector $\mathbf{u}$ that points from the receiver to the source. The signal originates in the far-field and may be considered to be a plane wave at the location of the receiver. Based on the received measurements, a DOA estimate $\hat{\mathbf{u}}$ (also being a unit vector) is produced.

A. Vector-sensor specification

The vector-sensor consists of a monopole sensor element, which is collocated with three dipole elements. The measurement of each sensor element can be expressed as $Ds[n]+e[n]$, where D is a directivity pattern, $s[n]$ is the signal, $e[n]$ signifies additive noise which may possibly induce error, and n represents discrete time. The monopole directivity pattern is uniform $D_{\text{mon}}=1$, and the dipole directivity pattern is: $D_{\text{dip}}=\mathbf{q}^T\mathbf{u}$, where $\mathbf{q}$ is a unit vector representing the orientation of the dipole. The dipole character of the latter expression follows directly from the definition of an inner product. The dipoles are oriented along the Cartesian axes: $\mathbf{q}_x=[1\ 0\ 0]^T$, $\mathbf{q}_y=[0\ 1\ 0]^T$ and $\mathbf{q}_z=[0\ 0\ 1]^T$. In the sequel, the monopole measurements will be represented by $p[n]$ and the dipoles measurements by $\mathbf{v}[n]=\left[v_x[n]\ v_y[n]\ v_z[n]\right]^T$ (corresponding to pressure and scaled particle-velocity from which these quantities may be obtained). From the previous discussion, the measured signals can be expressed as

$$p[n]=D_{\text{mon}}s[n]+e_p[n],$$

$$v_i[n]=\mathbf{q}_i^T\mathbf{u}s[n]+e_{v_i}[n],$$

where $e_p[n]$ is the additive monopole noise,

$$\mathbf{e}_v[n]=\left[e_{v_x}[n]\ e_{v_y}[n]\ e_{v_z}[n]\right]^T$$

is a vector comprising the additive noise of the three dipoles, and $i\in\{x,y,z\}$. Substituting the pertinent values, one obtains

$$p[n]=s[n]+e_p[n], \tag{1a}$$

$$v[n]=s[n]\mathbf{u}+\mathbf{e}_v[n]. \tag{1b}$$

B. Characterization of signal and noise

The signal $s[n]$ and noise components $e_p[n]$, $\mathbf{e}_v[n]$ are assumed to be independent identically distributed joint Gaussian processes. They have zero-mean and respective variances of σ_s^2, $\sigma_{e_p}^2$, and $\sigma_{e_v}^2$. Furthermore, the processes $s[n]$, $e_p[n]$, $e_{v_x}[n]$, $e_{v_y}[n]$, and $e_{v_z}[n]$ are all assumed to be mutually uncorrelated. The above-presented noise properties can be described succinctly as

$$E\left\{\begin{bmatrix} e_p[n] \\ \mathbf{e}_v[n] \end{bmatrix}\right\} = \mathbf{0}_{4\times 1}, \tag{2a}$$

$$E\left\{\begin{bmatrix} e_p[n] \\ \mathbf{e}_v[n] \end{bmatrix}\begin{bmatrix} e_p[n] \\ \mathbf{e}_v[n] \end{bmatrix}^T\right\} = \begin{bmatrix} \sigma_{e_p}^2 & \mathbf{0}_{1\times 3} \\ \mathbf{0}_{3\times 1} & \sigma_{e_v}^2 \cdot I_{3\times 3} \end{bmatrix}\delta[n-m], \tag{2b}$$

where $\mathbf{0}_{j\times k}$ and $\mathbf{I}_{j\times k}$, respectively, represent zero matrices and identity matrices of the designated dimensions, and $\delta[\circ]$ represents the Kronecker delta function.

Scenarios in which such noise characteristics can arise, comprise of settings containing internal[10] sensor noise and isotropic ambient noise.[23,24] Reverberative environments, do not subscribe to these characteristics,[1] and are not discussed in the present study.

The levels of internal sensor noise can be obtained from offline measurements. For ambient isotropic noise, it is known[23,24] that $\sigma_{e_p}^2/\sigma_{e_v}^2 = 3$. [It is subsequently shown in Eq. (18b) that knowledge of this ratio is sufficient for conducting ML estimation.] Alternatively, $\sigma_{e_p}^2$ and $\sigma_{e_v}^2$ may be estimated from noisy measurements using threshold detection methods, minimum statistics methods,[25] or a minimum mean-squared error noise tracking algorithm.[26]

C. Quantities for assessing estimation performance

The accuracy of DOA estimates can be evaluated by the angular error (AE), which is the angle by which $\hat{\mathbf{u}}$ deviates from $\mathbf{u}$, defined formally as[10,27]

$$\mathrm{AE} \equiv 2\sin^{-1}\left(\frac{\|\hat{\mathbf{u}}-\mathbf{u}\|}{2}\right), \tag{3}$$

where $\|\cdot\|$ is the Euclidian norm. The rate of convergence to the true value is described by the MSAE, which is defined as[10,27]

$$\mathrm{MSAE} \equiv \lim_{N\to\infty}(N\cdot E\{\mathrm{AE}^2\}), \tag{4}$$

where N is the number of discrete time instants measured. In the sequel, MSAE is presented in decibel units in order to facilitate comparison between different estimators and different scenarios.

III. MAXIMUM LIKELIHOOD ESTIMATION

In this section, we derive the probability density function (pdf) for sensor measurements taken over the course of N separate time instances ($0 \le n \le N-1$). We then determine the parameter $\mathbf{u}$, which corresponds to the maximum value of the pdf. This value of $\mathbf{u}$, which we call $\hat{\mathbf{u}}_{\mathrm{ML}}$, is the ML-DOA estimator.

Let $\mathbf{y}[n]$ be defined as the concatenation of monopole and dipole measurements: $\mathbf{y}[n] = [p[n]\ \mathbf{v}^T[n]]^T$. Substituting with Eq. (1) and using the specifications of Sec. II B, the value of the covariance matrix $\mathbf{C} = \mathrm{Cov}\{y[n]\}$ can be derived as

$$\mathbf{C} = \begin{bmatrix} \sigma_{e_p}^2 & & & \\ & \sigma_{e_v}^2 & & \\ & & \sigma_{e_v}^2 & \\ & & & \sigma_{e_v}^2 \end{bmatrix} + \sigma_s^2\begin{bmatrix} 1 \\ \mathbf{u} \end{bmatrix}\begin{bmatrix} 1 \\ \mathbf{u} \end{bmatrix}^T, \tag{5}$$

where the omitted off-diagonal elements are to be taken as zeros. Also, according to the specifications it is assumed that $\mathbf{y}[n]$ and $\mathbf{y}[m]$ are statistically independent for $n \ne m$. Hence, the pdf of $\mathbf{y}[n]$ for $0 \le n \le N-1$ is

$$f_{\mathbf{y}[n]}(\mathbf{y}[n]) = \frac{1}{(2\pi)^{N/2}|\mathbf{C}|^{1/2}}\prod_{n=0}^{N-1}\exp\left\{-\frac{1}{2}\mathbf{y}^T[n]\mathbf{C}^{-1}\mathbf{y}[n]\right\}. \tag{6}$$

In order to obtain the maximum likelihood DOA estimation, we must find a feasible $\mathbf{u}$ that maximizes Eq. (6), that is

$$\hat{\mathbf{u}}_{\mathrm{ML}} = \underset{\mathbf{u}}{\mathrm{argmax}}\ \{f_{\mathbf{y}[n]}(\mathbf{y}[n])\} \quad \text{subject to} \quad \mathbf{u}^T\mathbf{u} = 1. \tag{7}$$

The pdf (6), which we wish to maximize with respect to $\mathbf{u}$, contains the matrix $\mathbf{C}$, which is dependent on $\mathbf{u}$; all other terms are independent of $\mathbf{u}$. This matrix occurs twice and in two guises: First in the form of a determinant, and then in the form of a matrix inverse. The decomposition of $\mathbf{C}$ into simpler elements facilitates the solution of Eq. (7). We can write Eq. (5) as $\mathbf{C} = \mathbf{C}_e + \mathbf{C}_s$, where $\mathbf{C}_e = \mathrm{diag}([\sigma_{e_p}^2\ \ \sigma_{e_v}^2\ \ \sigma_{e_v}^2\ \ \sigma_{e_v}^2])$ is a diagonal noise matrix and $\mathbf{C}_s = \sigma_s^2[1\ \ \mathbf{u}^T]^T[1\ \ \mathbf{u}^T]$ is a rank one signal matrix. The signal matrix $\mathbf{C}_s$ can, in turn, be expressed as the outer product $\mathbf{b}\mathbf{b}^T$ of the column vector

$$\mathbf{b} = \begin{bmatrix} \sigma_s \\ \sigma_s\mathbf{u} \end{bmatrix}. \tag{8}$$

Therefore, we can write the covariance matrix $\mathbf{C}$ as

$$\mathbf{C} = \mathbf{C}_e + \mathbf{C}_s = \mathbf{C}_e + \mathbf{b}\mathbf{b}^T. \tag{9}$$

The determinant $|\mathbf{C}| = |\mathbf{C}_e + \mathbf{b}\mathbf{b}^T|$ can be evaluated through the matrix determinant lemma[28] as $|\mathbf{C}_e|(1+\mathbf{b}^T\mathbf{C}_e^{-1}\mathbf{b})$. The term $|\mathbf{C}_e|$ is independent of $\mathbf{u}$. Furthermore, the second multiplicand may be reconstructed as

$$1+\mathbf{b}^T\mathbf{C}_e^{-1}\mathbf{b} = 1+\sigma_s^2\left(\sigma_{e_p}^{-2}+\sigma_{e_v}^{-2}\right), \tag{10}$$

which is also independent of $\mathbf{u}$. Consequently, $|\mathbf{C}|$ is constant with respect to $\mathbf{u}$.

Therefore, optimization problem (7) can now be converted into an equivalent form as follows:

$$\hat{\mathbf{u}}_{ML} = \underset{\mathbf{u}}{\mathrm{argmax}}\left\{-\sum_{n=0}^{N-1}\mathbf{y}^T[n]\mathbf{C}^{-1}\mathbf{y}[n]\right\} \quad \text{s.t.} \quad \mathbf{u}^T\mathbf{u} = 1, \tag{11}$$

by applying a logarithm to the target function of Eq. (6) and eliminating constants. The inverse matrix $\mathbf{C}^{-1} = (\mathbf{C}_e + \mathbf{b}\mathbf{b}^T)^{-1}$ may be reformulated through the matrix inversion lemma[29] as

$$\left(\mathbf{C}_e + \mathbf{b}\mathbf{b}^T\right)^{-1} = \mathbf{C}_e^{-1} - \frac{\mathbf{C}_e^{-1}\mathbf{b}\mathbf{b}^T\mathbf{C}_e^{-1}}{1 + \mathbf{b}^T\mathbf{C}_e^{-1}\mathbf{b}}. \tag{12}$$

The first term $\mathbf{C}_e^{-1}$ is independent of $\mathbf{u}$ and the denominator of the second term is independent of $\mathbf{u}$, as well [see Eq. (10)]. Thus, Eq. (11) can be modified to the equivalent,

$$\hat{\mathbf{u}}_{ML} = \underset{\mathbf{u}}{\operatorname{argmax}} \left\{ \sum_{n=0}^{N-1} \mathbf{y}^T[n]\mathbf{C}_e^{-1}\mathbf{b}\mathbf{b}^T\mathbf{C}_e^{-1}\mathbf{y}[n] \right\} \quad \text{s.t.} \quad \mathbf{u}^T\mathbf{u} = 1. \tag{13}$$

The target function (i.e., the term in curly braces) of Eq. (13) can be reordered as

$$\mathbf{b}^T\mathbf{C}_e^{-1} \left(\sum_{n=0}^{N-1} \mathbf{y}[n]\mathbf{y}^T[n] \right) \mathbf{C}_e^{-1}\mathbf{b}, \tag{14}$$

and cast into block matrix form as

$$N \begin{bmatrix} \sigma_{e_p}^{-2} \\ \sigma_{e_v}^{-2}\mathbf{u} \end{bmatrix}^T \begin{bmatrix} \hat{r}_{pp} & \hat{\mathbf{r}}_{pv}^T \\ \hat{\mathbf{r}}_{pv} & \hat{\mathbf{R}}_{vv} \end{bmatrix} \begin{bmatrix} \sigma_{e_p}^{-2} \\ \sigma_{e_v}^{-2}\mathbf{u} \end{bmatrix}, \tag{15}$$

where $\hat{r}_{pp}$, $\hat{\mathbf{r}}_{pv}^T$, and $\hat{\mathbf{R}}_{vv}$ are the respective sample-averaged second moment terms,

$$\hat{r}_{pp} = \frac{1}{N}\sum_{n=0}^{N-1} p^2[n], \tag{16a}$$

$$\hat{\mathbf{r}}_{pv} = \frac{1}{N}\sum_{n=0}^{N-1} \mathbf{v}[n]p[n], \tag{16b}$$

$$\hat{\mathbf{R}}_{vv} = \frac{1}{N}\sum_{n=0}^{N-1} \mathbf{v}[n]\mathbf{v}^T[n]. \tag{16c}$$

Discarding the constant N and performing the block matrix multiplication, Eq. (15) becomes

$$\sigma_{e_p}^{-4}\hat{r}_{pp} + 2\sigma_{e_p}^{-2}\sigma_{e_v}^{-2}\mathbf{u}^T\hat{\mathbf{r}}_{pv} + \sigma_{e_v}^{-4}\mathbf{u}^T\hat{\mathbf{R}}_{vv}\mathbf{u}. \tag{17}$$

We produce a more convenient form by dropping the term $\sigma_{e_p}^{-4}\hat{\mathbf{r}}_{pp}$, which is a constant (with respect to $\mathbf{u}$) and subsequently multiplying by $(\sigma_{e_p}^2\sigma_{e_v}^4)/[2(\sigma_{e_p}^2 + \sigma_{e_v}^2)]$. The resulting target function $T_{\mathrm{ML}}(\mathbf{u})$ is equivalent to that of Eq. (13) and is expressed as

$$T_{\mathrm{ML}}(\mathbf{u}) = \alpha_0\mathbf{u}^T\hat{\mathbf{r}}_{pv} + (1-\alpha_0)\frac{1}{2}\mathbf{u}^T\hat{\mathbf{R}}_{vv}\mathbf{u}, \tag{18a}$$

where

$$\alpha_0 = \frac{\sigma_{e_v}^2}{\sigma_{e_p}^2 + \sigma_{e_v}^2}. \tag{18b}$$

Maximization of $T_{\mathrm{ML}}(\mathbf{u})$ subject to the unity constraint,

$$\hat{\mathbf{u}}_{\mathrm{ML}} = \underset{\mathbf{u}}{\operatorname{argmax}} \{T_{\mathrm{ML}}(\mathbf{u})\} \quad \text{s.t.} \quad \mathbf{u}^T\mathbf{u} = 1, \tag{19}$$

yields the maximum likelihood DOA estimator defined in Eq. (7). The significance of the constant α_0 defined in Eq. (18b) is addressed in the following section.

IV. MAXIMUM-SRP DOA ESTIMATION AND MINIMUM POWER BEAMFORMING

In this section, we present an alternative approach for DOA estimation that is based on steering a given beampattern toward the direction providing maximum SRP. The ML-DOA estimator is shown to be tantamount to a particular instance of this approach, which selects the optimal beampattern. Afterwards, we demonstrate a relationship between the ML-DOA estimator and the MPDR beamformer.

A. DOA estimation by steering to direction of maximum SRP

A first-order beamformer, which consists of a weighted sum of monopole and dipole elements, produces the following signal:

$$y_{\mathrm{b}}[n] = \alpha p[n] + (1-\alpha)\mathbf{u}_{\mathrm{b}}^T\mathbf{v}[n], \tag{20}$$

where $\mathbf{u}_b$ represents the look direction, and the parameter α determines the proportionate weight of the monopole and dipole components. Note that Eq. (20) has been formulated such that the response in the look direction is constrained to unity. Furthermore, requiring that $\alpha \in [0, 1]$ ensures that the response in the look direction is maximal. The beampatterns produced by the above-mentioned arrangement are known as limaçons. The specific choices of α being 0, 0.5, and 1, respectively, produce dipole, cardioid, and monopole patterns.

The power of a received signal $(1/N)\sum_{n=0}^{N-1} y_{\mathrm{b}}^2[n]$ is dependent on both α and $\mathbf{u}_{\mathrm{b}}$. When α is held constant and the look direction is steered toward the true DOA, the average power tends to increase. Using this observation, a maximum-SRP DOA estimator $\hat{\mathbf{u}}_{\mathrm{MSRP}}$, which is dependent on α can be defined as

$$\hat{\mathbf{u}}_{\mathrm{MSRP}}(\alpha) = \underset{\mathbf{u}_{\mathrm{b}}}{\operatorname{argmax}} \left\{ \frac{1}{N}\sum_{n=0}^{N-1} \left(\alpha p[n] + (1-\alpha)\mathbf{u}_{\mathrm{b}}^T\mathbf{v}[n]\right)^2 \right\} \quad \text{s.t.} \quad \mathbf{u}_{\mathrm{b}}^T\mathbf{u}_b = 1. \tag{21}$$

It can be shown[20] that the target function (term in curly braces) of Eq. (21) can be cast into an equivalent form as follows:

$$T_{\mathrm{MSRP}}(\mathbf{u}_{\mathrm{b}}) = \alpha\mathbf{u}_{\mathrm{b}}^T\hat{\mathbf{r}}_{pv} + (1-\alpha)\frac{1}{2}\mathbf{u}_{\mathrm{b}}^T\hat{\mathbf{R}}_{vv}\mathbf{u}_{\mathrm{b}}. \tag{22}$$

If we choose $\alpha = 0$, the beampattern is shaped as a dipole, and $\hat{\mathbf{u}}_{\mathrm{MSRP}}(0)$ coincides with the eigenvector of $\hat{\mathbf{R}}_{vv}$ corresponding to the largest eigenvalue.[30] Nehorai and Paldi[10] presented an estimator identical to $\hat{\mathbf{u}}_{\mathrm{MSRP}}(0)$ under the name

Velocity-Covariance-Based Algorithm. For $\alpha \to 1^-$ (i.e., approaching 1 from below), we obtain a near-monopole pattern with $\hat{\mathbf{u}}_{\mathrm{MSRP}}(1^-) = \hat{\mathbf{r}}_{pv}/\|\hat{\mathbf{r}}_{pv}\|$. An estimator corresponding to $\hat{\mathbf{u}}_{\mathrm{MSRP}}(1^-)$ was presented by Nehorai and Paldi[10] under the name *Intensity-Based Algorithm* and an earlier work by Davies[22] presented this solution for a two-dimensional scenario. In summary, these two independently developed algorithms are special cases of the maximum SRP approach.

For the intermediate case where $0 < \alpha < 1$, no direct analytical solution to Eq. (21) is evident. In Ref. 20 we presented an iterative algorithm incorporating constrained gradient ascent (resembling that of Cox *et al.*[31]) which approaches the solution and is computationally inexpensive (the details of this algorithm are summarized in the Appendix). It was shown experimentally that estimation accuracy (as measured by MSAE) is dependent on the beampattern parameter α together with the signal and noise variances (σ_s^2, $\sigma_{e_p}^2$, and $\sigma_{e_v}^2$). For certain intermediate values of α, a reduced MSAE was obtained which was smaller than those of both $\hat{\mathbf{u}}_{\mathrm{MSRP}}(1^-)$ and $\hat{\mathbf{u}}_{\mathrm{MSRP}}(0)$. Furthermore, with α properly chosen, the resulting MSAE was seen to approach the analytically derived[10] CRLB. However, it is not immediately apparent which value for α will produce optimal results.

Comparison of Eqs. (18a) and (22) reveals that the target functions $T_{\mathrm{ML}}(\mathbf{u})$ and $T_{\mathrm{MSRP}}(\mathbf{u})$ subscribe to the same form. Specifically, $T_{\mathrm{ML}}(\mathbf{u})$ is essentially the target function of a maximum-SRP DOA estimator where the beampattern parameter is $\alpha = \alpha_0$ [as defined in Eq. (18b)]. Thus, the maximum likelihood DOA estimator $\hat{\mathbf{u}}_{\mathrm{ML}}$ amounts to a special case of the maximum-SRP DOA estimator. The uniqueness of this case lies in the fact that ML estimators possess the property of asymptotic efficiency,[32] and thus $\hat{\mathbf{u}}_{\mathrm{ML}}$ achieves the CRLB.

B. Minimum power distortionless response beamforming

We now consider a somewhat different problem in the realm of spatial signal processing, which is the problem of signal enhancement through beamforming. DOA estimation and signal enhancement may be viewed as complementary problems. Namely, noise inhibits the estimation of DOA in the former, whereas in the latter the DOA is known and the goal is elimination of noise.

We now describe the problem of signal enhancement through beamforming in more detail. Consider a scenario in which the direction $\mathbf{u}$ is known. The goal is to estimate $s[n]$ as a weighted combination of the available measurements, i.e.,

$$\hat{s}[n] = \mathbf{w}^T \mathbf{y}[n]. \tag{23}$$

The measurements can be represented as $\mathbf{y}[n] = \mathbf{h}s[n] + \mathbf{e}[n]$, where $\mathbf{h} = [1 \quad \mathbf{u}^T]^T$ is the array-manifold corresponding to the correct DOA, and $\mathbf{e}[n] = [e_p[n] \quad \mathbf{e}_v^T[n]]^T$ [see Eq. (1)]. The estimate should maintain a unit signal response while containing minimal power (and hence reduced noise).[33] More formally,

$$\mathbf{w}_{\mathrm{MPDR}} = \underset{\mathbf{w}}{\operatorname{argmin}}\, \mathbf{w}^T \mathbf{C} \mathbf{w} \qquad \text{s.t.} \quad \mathbf{w}^T \mathbf{h} = 1. \tag{24}$$

The well-known solution[34] to Eq. (24) is

$$\mathbf{w}_{\mathrm{MPDR}} = \frac{\mathbf{C}^{-1}\mathbf{h}}{\mathbf{h}^T \mathbf{C}^{-1} \mathbf{h}}. \tag{25}$$

Applying Eq. (25) with the pertinent values for $\mathbf{C}$ and $\mathbf{h}$ produces

$$\mathbf{w}_{\mathrm{MPDR}} = \begin{bmatrix} \alpha_0 \\ (1-\alpha_0)\mathbf{u} \end{bmatrix}, \tag{26}$$

where α_0 is given by Eq. (18b). Substitution of Eq. (26) into Eq. (23) yields an output signal as follows:

$$\hat{s}[n] = \alpha_0 p[n] + (1-\alpha_0)\mathbf{u}^T \mathbf{v}[n]. \tag{27}$$

The MPDR beamformer of Eq. (27) conforms to the mold of Eq. (20) with the look direction $\mathbf{u}_{\mathrm{b}}$ specified as $\mathbf{u}$ (the true DOA) and the shape parameter α specified as α_0 (the optimal parameter for maximum-SRP DOA estimation). This result can be interpreted as a duality between maximum-SRP DOA estimation in which power is *maximized* [Eq. (21)] and MPDR beamforming in which power is *minimized* [Eq. (24)]—both cases obtain optimality with the same shape parameter.

It should be noted that, in general, the direction of maximum SRP of an MPDR beam-former and the ML-DOA estimator are *not* identical.[35] The equivalence exhibited previously results from the particular structures of the noise matrix $\mathbf{C}_e$ and the array manifold $\mathbf{h}$. A similar result can also be shown to hold in the case of a narrowband far-field source received by an array of monopole sensors with a corresponding diagonal noise matrix.

V. PERFORMANCE

The accuracy of the various DOA estimators may be gauged by their MSAE. In Ref. 10 analytic terms for the MSAE of the dipole estimator $\hat{\mathbf{u}}_{\mathrm{MSRP}}(0)$ and near monopole estimator $\hat{\mathbf{u}}_{\mathrm{MSRP}}(1^-)$ were calculated, as well as the CRLB. The results are reproduced here in a slightly different form and are adapted for time domain measurements (as opposed to phasor measurements in the original work):

$$\mathrm{MSAE}_{\hat{\mathbf{u}}_{\mathrm{MSRP}}(1^-)} = 2\frac{\sigma_{e_v}^2}{\sigma_s^2}\left(1 + \frac{\sigma_{e_v}^2}{\sigma_s^2}\right), \tag{28a}$$

$$\mathrm{MSAE}_{\hat{\mathbf{u}}_{\mathrm{MSRP}}(0)} = 2\frac{\sigma_{e_v}^2}{\sigma_s^2}\left(1 + \frac{\sigma_{e_v}^2}{\sigma_s^2}\right), \tag{28b}$$

$$\mathrm{MSAE}_{\mathrm{CRLB}} = 2\frac{\sigma_{e_v}^2}{\sigma_s^2}\left(1 + \frac{\sigma_{e_p \| e_v}^2}{\sigma_s^2}\right). \tag{28c}$$

The symbol $\sigma_{e_p \| e_v}^2$ denotes the following quantity: $\sigma_{e_p \| e_v}^2 = (\sigma_{e_p}^{-2} + \sigma_{e_v}^{-2})^{-1}$. Maximum likelihood estimators are known

to be asymptotically efficient.[32] Consequently, the MSAE of $\hat{\mathbf{u}}_{\mathrm{ML}} = \hat{\mathbf{u}}_{\mathrm{MSRP}}(\alpha_0)$ is that described in Eq. (28c).

In order to compare the performance of the different estimators, Monte Carlo simulations were performed to produce sample MSAE values. For each test, a total of MC = 100 000 DOA estimation scenario trials were created. The procedure used is as follows: First, a DOA $\mathbf{u}$ was generated on a random basis. Afterwards, the source and noise signals $s[n]$, $e_p[n]$, and $\mathbf{e}_v[n]$ were drawn from independent zero-mean Gaussian distributions with respective variances σ_s^2, $\sigma_{e_p}^2$, and $\sigma_{e_v}^2$. These signals were used to create the sensor measurements $p[n]$ and $\mathbf{v}[n]$, as described in Eq. (1). The length of the signals used in our simulation was $N = 80\,000$. The maximum-SRP DOA estimators with α ranging from 0 to 1, were computed by solving Eq. (21) by means of the algorithm presented in Ref. 20 (see the Appendix). The AE pertaining to each estimator was calculated according to Eq. (3), and after the completion of the MC trials these results were used to calculate the sample MSAE. In Fig. 1 the results of three such simulations are presented. The solid curve represents the maximum-SRP DOA estimation and the dashed line represents the CRLB term described in Eq. (28c). Particular points of interest are also marked: The analytically calculated MSAE values of dipole and near-monopole algorithms [Eqs. (28a) and (28b)] are marked, respectively, by a diamond and by a square. The five pointed star represents the sample MSAE of the ML estimator.

Examination of Fig. 1 clearly demonstrates the advantages of using an ML estimator over other maximum SRP estimators in terms of reduced MSAE. The MSAE of the dipole and near-monopole estimators are represented by the upper outward tips of the maximum-SRP curve (at $\alpha = 0$ and $\alpha \to 1^-$). At intermediate values of α, a reduction of MSAE is obtained. The minimum of the curve occurs at $\alpha = \alpha_0$, which corresponds to the ML-DOA estimator. The MSAE of this estimator coincides with the CRLB indicating asymptotic efficiency.

The best selection of parameter α and the reduction in MSAE obtained therefrom is highly dependent upon the power levels of signal and noise components pertaining to a particular scenario. For example, in Fig. 1(a) the signal and noise variances are: $\sigma_s^2 = 0.5$, $\sigma_{e_p}^2 = 0.7$, and $\sigma_{e_v}^2 = 1.3$. The optimal parameter is $\alpha_0 = 0.65$, which achieves the lower bound $\mathrm{MSAE}_{\mathrm{CRLB}} = 9.97$ dB. This improves upon $\mathrm{MSAE}_{\hat{\mathbf{u}}_{\mathrm{MSRP}}(0)} = 12.723$ dB and $\mathrm{MSAE}_{\hat{\mathbf{u}}_{\mathrm{MSRP}}(1^-)} = 10.926$ dB. In Fig. 1(b) ($\sigma_s^2 = 2$, $\sigma_{e_p}^2 = 6$, $\sigma_{e_v}^2 = 2$) the optimal parameter $\alpha_0 = 0.25$ achieves the lower bound of $\mathrm{MSAE}_{\mathrm{CRLB}} = 5.441$ dB in contrast to $\mathrm{MSAE}_{\hat{\mathbf{u}}_{\mathrm{MSRP}}(0)} = 6.021$ dB, and $\mathrm{MSAE}_{\hat{\mathbf{u}}_{\mathrm{MSRP}}(1^-)} = 9.031$ dB. Finally in Fig. 1(c) ($\sigma_s^2 = 1$, $\sigma_{e_p}^2 = 10$, $\sigma_{e_v}^2 = 10$), the optimal parameter is $\alpha_0 = 0.5$, which achieves the lower bound $\mathrm{MSAE}_{\mathrm{CRLB}} = 20.792$ dB, which improves upon $\mathrm{MSAE}_{\hat{\mathbf{u}}_{\mathrm{MSRP}}(0)} = \mathrm{MSAE}_{\hat{\mathbf{u}}_{\mathrm{MSRP}}(1^-)} = 23.424$.

The optimal beampatterns pertaining to the aforementioned cases are plotted in Fig. 2. The look direction is taken as 0° and the polar curve corresponds to received power (i.e., the amplitude response squared). It should be noted that the beampattern determined by Eq. (18b) is independent of signal power σ_s^2. When $\sigma_{e_v}^2 > \sigma_{e_p}^2$ the limaçon is subcardioid,

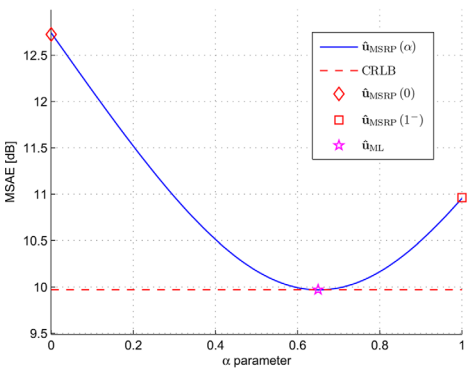

(a) $\sigma_s^2 = 0.5$, $\sigma_{e_p}^2 = 0.7$, $\sigma_{e_v}^2 = 1.3$

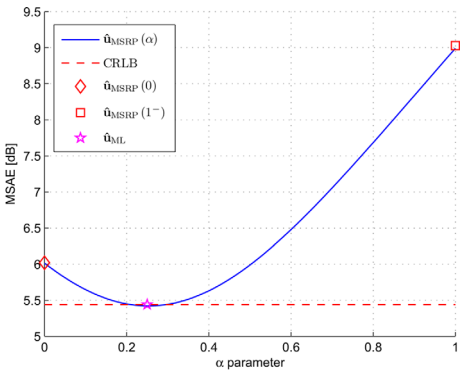

(b) $\sigma_s^2 = 2$, $\sigma_{e_p}^2 = 6$, $\sigma_{e_v}^2 = 2$

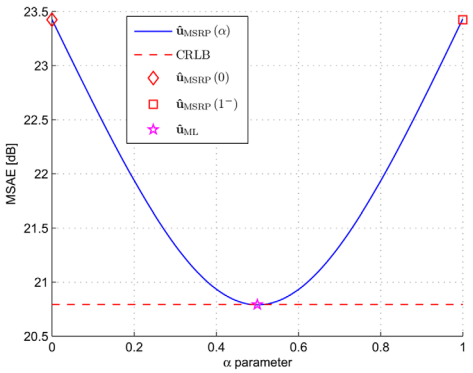

(c) $\sigma_s^2 = 1$, $\sigma_{e_p}^2 = 10$, $\sigma_{e_v}^2 = 10$

FIG. 1. (Color online) Comparison of sample MSAE for maximum-SRP DOA estimation with different beampattern parameters α in the range [0, 1). The dipole and near-monopole estimators ($\alpha = 0$ and $\alpha = 1^-$, respectively), as well as the ML-DOA estimator are special cases. The MSAE of the ML-DOA estimator coincides with the CRLB.

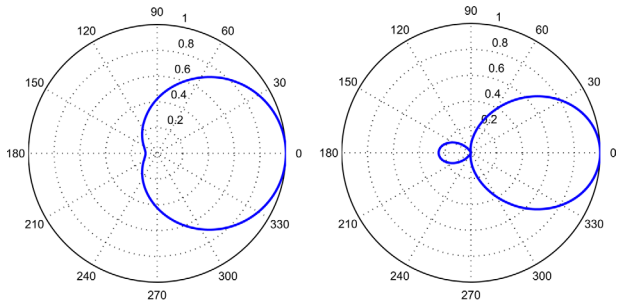

(a) $\alpha = 0.65$ (b) $\alpha = 0.25$

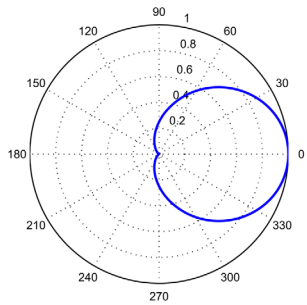

(c) $\alpha = 0.5$

FIG. 2. (Color online) Optimal beampatterns relating to (a) $\sigma_{e_p}^2 = 0.7$, $\sigma_{e_v}^2 = 1.3$, (b) $\sigma_{e_p}^2 = 6$, $\sigma_{e_v}^2 = 2$, and (c) $\sigma_{e_p}^2 = \sigma_{e_v}^2 = 10$.

when $\sigma_{e_v}^2 < \sigma_{e_p}^2$ the limaçon is supercardioid, and when $\sigma_{e_v}^2 = \sigma_{e_p}^2$ the limaçon is a cardioid. This is depicted in Fig. 2(a), which is subcardioid ($\alpha = 0.65$), in Fig. 2(b), which is supercardioid ($\alpha = 0.25$), and in Fig. 2(c), which is cardioid ($\alpha = 0.5$).

To further illustrate the relationships between estimation performance and signal and noise power levels, a number of scenarios are listed in Table I. First, we note that multiplication of the *three* parameters (σ_s^2, $\sigma_{e_p}^2$, $\sigma_{e_p}^2$) by a common scaling factor has no effect on estimation performance [Eqs. (28a)–(28c) are invariant to scaling]. Hence, a scenario can be specified by the *two* signal-to-noise ratio (SNR) parameters $\sigma_s^2/\sigma_{e_p}^2$ and $\sigma_s^2/\sigma_{e_p}^2$ corresponding to monopole-SNR and dipole-SNR, respectively. For each scenario of Table I, the monopole-SNR and dipole-SNR are listed. The MSAE is calculated for $\hat{\mathbf{u}}_{\mathrm{MSRP}}(0)$, $\hat{\mathbf{u}}_{\mathrm{MSRP}}(1^-)$, and $\hat{\mathbf{u}}_{\mathrm{ML}}$ according to (28), which provides analytically derived values. The optimal beam-pattern parameter α_0 used to produce $\hat{\mathbf{u}}_{\mathrm{ML}}$ is calculated according to (18b). Finally the reduction in MSAE attainable by use of the ML-DOA estimator is presented under the column entitled "ML-gain." We define this as the relative improvement in MSAE afforded by the ML-DOA estimator with respect to the better of the two estimators $\hat{\mathbf{u}}_{\mathrm{MSRP}}(0)$ and $\hat{\mathbf{u}}_{\mathrm{MSRP}}(1^-)$, or more formally as the following ratio:

$$\text{ML-gain} = \frac{\mathrm{MSAE}_{\mathrm{CRLB}}}{\min\left\{\mathrm{MSAE}_{\hat{\mathbf{u}}_{\mathrm{MSRP}}(0)}, \mathrm{MSAE}_{\hat{\mathbf{u}}_{\mathrm{MSRP}}(1^-)}\right\}}. \quad (29)$$

The SNR parameters as well as the different MSAEs and the ML-gain are all given in decibels (dB).

The first two rows (a and b) correspond to the cases presented in Figs. 1(a) and 1(b), respectively. The rest of the chart refers to various scenarios in which the monopole SNR is -10, 0, and 10 dB, [corresponding to poor SNR (rows c–f), moderate SNR (rows g–j), and high SNR (rows k–n)]. Each of these cases is examined for situations in which the difference between the monopole and dipole SNRs are 10, 0, -4.77, and -10 dB. These relationships correspond, respectively, to cases where dipole noise dominates, dipole and monopole noises maintain equal power, monopole noises dominate, and the noise is of an isotropic nature[23,24] with a 3:1 ratio (4.77 dB). [Note that row d corresponds to the case presented in Fig. 1(c).]

Several observations are illustrated in the tabulated scenarios, which may be divided into three cases. (1) When monopole noise dominates ($\sigma_{e_p}^2 \gg \sigma_{e_v}^2$) (f, j, n) then the optimal beampattern is nearly dipole ($\alpha_0 = 0.091$), and the ML-gain indicates only a minor improvement. (2) Similarly, when dipole noise dominates ($\sigma_{e_p}^2 \ll \sigma_{e_v}^2$) (c, g, k) then the optimal beampattern is nearly monopole ($\alpha_0 = 0.909$), and the ML-gain indicates only a minor improvement. (3) However, when the monopole noise and dipole noise are of equal value (d, h, l) or of similar magnitude (a, b, e, i, m), then the optimal beampattern is not a near-monopole or near-dipole (but rather lies somewhere in between). In these scenarios, higher ML-gains are possible depending on the SNR levels. For high SNRs (e.g., scenarios l and m), all three estimators exhibit roughly the same performance and the ML-gain is negligible. This is also evident from the fact that the parenthesized terms, which distinguish Eqs. (28a), (28b), and (28c), all equal unity to a good approximation. Conversely, for modest and especially for low SNRs, a more significant ML-gain is possible (e.g., scenarios d and h). The supremum of ML-gain [i.e., the supremum of Eq. (29) with respect to all allowable combinations of σ_s^2, $\sigma_{e_p}^2$, and $\sigma_{e_p}^2$] can be shown to be 2 ($\approx$3 dB). This occurs when $\sigma_{e_p}^2 = \sigma_{e_v}^2 \gg \sigma_s^2$. (Compare with row d of Table I, which approaches these specifications and attains an ML-gain of 2.632 dB.)

TABLE I. Performance of different DOA estimators and optimal beampattern parameter (α_0) corresponding to scenarios with varying signal power levels and noise levels of monopole and dipole elements.

	SNRs (dB)		MSAE (dB)				
	$\sigma_s^2/\sigma_{e_p}^2$	$\sigma_s^2/\sigma_{e_v}^2$	$\hat{\mathbf{u}}_{\mathrm{MSRP}}(0)$	$\hat{\mathbf{u}}_{\mathrm{MSRP}}(1^-)$	$\hat{\mathbf{u}}_{\mathrm{ML}}$	α_0	ML-gain (dB)
(a)	−1.461	−4.150	12.723	10.962	9.970	0.650	0.992
(b)	−4.771	0	6.021	9.031	5.441	0.250	0.580
(c)	−10	−20	43.054	33.424	33.050	0.909	0.375
(d)	−10	−10	23.424	23.424	20.792	0.500	2.632
(e)	−10	−5.229	14.607	18.653	13.680	0.250	0.928
(f)	−10	0	6.021	13.424	5.819	0.091	0.202
(g)	0	−10	23.424	16.021	15.819	0.909	0.202
(h)	0	0	6.021	6.021	4.771	0.500	1.249
(i)	0	4.771	−0.512	1.249	−0.792	0.250	0.280
(j)	0	10	−6.576	−3.979	−6.612	0.091	0.036
(k)	10	0	6.021	3.424	3.388	0.909	0.036
(l)	10	10	−6.576	−6.576	−6.778	0.500	0.202
(m)	10	14.771	−11.619	−11.347	−11.654	0.250	0.035
(n)	10	20	−16.946	−16.576	−16.950	0.091	0.004

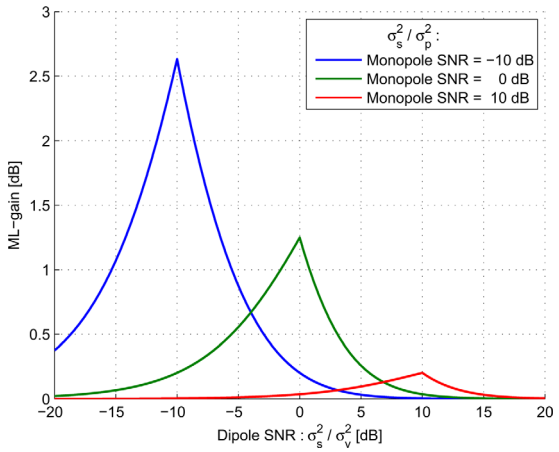

FIG. 3. (Color online) The ML-gain from Eq. (29) plotted for various SNR parameters. The gain is most tangible for cases having low SNR and monopole and dipole noise levels of similar magnitude.

Figure 3 illustrates the ML-gain for different SNR parameters. The three curves depict ML-gain as a function of dipole SNR and correspond to monopole SNRs of −10, 0, and 10 dB. The ML-gain exhibits sharp peaks when the dipole and monopole SNRs are equal. Peak level values increase as SNR decreases.

In practical applications, the current state of particle-velocity sensors is not mature in comparison to conventional pressure sensors, which are well established. Hence, dipole noise can be expected to dominate in devices containing particle-velocity sensors. With respect to isotropic noise originating from the environment, monopole noise is stronger than dipole noise with a 3:1 ratio,[23,24] but does not dominate by an order of magnitude (i.e., $\sigma_{e_p}^2 \gg \sigma_{e_v}^2$ is not a valid description). The optimal beampattern parameter is $\alpha_0 = 0.25$ admitting a tangible ML-gain

VI. SUMMARY

In this work we proposed a maximum likelihood-based DOA estimator for a single vector-sensor in the presence of an isotropic noise field. Vector-sensors provide more information about a given sound field than conventional pressure sensors do. Thus, incorporation of vector-sensors in signal processing applications can yield enhanced performance. Whereas a single vector-sensor is inherently directional and can be used for DOA estimation, an unidirectional pressure sensor lacks this quality, and multiple sensors are required for the aforementioned task.

The proposed ML estimator is a specific realization of the maximum-SRP DOA estimation with an optimal choice of beampattern parameter. In an earlier contribution, we showed that the family of maximum-SRP estimators generalizes two previously proposed estimators (namely, the Intensity-Based Algorithm and Velocity-Covariance-Based Algorithm) and can surpass their performance in terms of MSAE. These estimators can be calculated in a computationally inexpensive manner. However, it was not clear which member of the aforementioned family obtains optimal performance. In the current work we showed that the ML-DOA estimator constitutes the optimal choice of beampattern and achieves the CRLB. The beampattern of the ML-DOA estimator is shared with that of the MPDR beamformer. This immediately suggests the possibility of performing DOA steering in conjunction with signal enhancement under a joint framework.

The improvement in MSAE, which is attainable due to ML-DOA estimation, is dependent on the monopole and dipole SNRs of each particular scenario. The improvement is most pronounced in low SNR scenarios in which the monopole and dipole noise levels are of similar magnitude. The ML-gain is bounded by a supremum of a 3 dB improvement.

APPENDIX: ITERATIVE GRADIENT BASED ALGORITHM FOR SRP MAXIMIZATION

In this appendix, we present a brief sketch of the algorithm presented in Ref. 20 for SRP maximization. We wish to maximize the target function $T_{\mathrm{MSRP}}(\mathbf{u}_\mathrm{b})$ defined in Eq. (22) subject to the constraint of unity vector-length. Formally stated,

$$\hat{\mathbf{u}}_{\mathrm{MSRP}}(\alpha) = \underset{\mathbf{u}_\mathrm{b}}{\operatorname{argmax}} \left\{ \alpha \mathbf{u}_\mathrm{b}^T \hat{\mathbf{r}}_{pv} + (1-\alpha)\frac{1}{2}\mathbf{u}_\mathrm{b}^T \hat{\mathbf{R}}_{vv}\mathbf{u}_\mathrm{b} \right\} \quad \text{s.t. } \mathbf{u}_\mathrm{b}^T\mathbf{u}_\mathrm{b} = 1. \tag{A1}$$

The proposed iterative algorithm is based on the principle of gradient ascent. The gradient of the target function is

$$\nabla_{\mathbf{u}_\mathrm{b}} T_{\mathrm{MSRP}}(\mathbf{u}_\mathrm{b}) = \alpha\hat{\mathbf{r}}_{pv} + (1-\alpha)\hat{\mathbf{R}}_{vv}\mathbf{u}_\mathrm{b}. \tag{A2}$$

Starting with some initial vector $\mathbf{u}_{\mathrm{b}_0}$, a perturbation in the direction of the gradient tends to increase the value of the target function. As the perturbed vector is likely to violate the unity constraint in (A1), normalization is performed after each perturbation.

The algorithm can be conveniently initialized with the Intensity-Based Algorithm $\mathbf{u}_{\mathrm{b}0} = \hat{\mathbf{r}}_{pv}/\|\hat{\mathbf{r}}_{pv}\| = \hat{\mathbf{u}}_{\mathrm{MSRP}}(1^-)$. Alternatively, the initial vector can be set as a normalized combination of $\hat{\mathbf{u}}_{\mathrm{MSRP}}(1^-)$ and $\hat{\mathbf{u}}_{\mathrm{MSRP}}(0)$. The algorithm can be set to terminate either after a fixed number of steps or when the change induced by the current step is less than a given threshold: $\|\mathbf{u}_{\mathrm{b}_{\mathrm{current}}} - \mathbf{u}_{\mathrm{b}_{\mathrm{previous}}}\|^2 < \epsilon^2$. The algorithm is summarized in the schematic entitled Algorithm 1.

Algorithm 1. Iterative algorithm for finding direction of maximum power.
Input: $\hat{\mathbf{R}}_{vv}$, $\hat{\mathbf{r}}_{pv}$, α
$\mathbf{u}_{\mathrm{b}_0} := \hat{\mathbf{u}} = \hat{\mathbf{r}}_{pv}/\|\hat{\mathbf{r}}_{pv}\|$
$k := 0$
$K :=$ maximum number of iterations
$\epsilon :=$ tolerance parameter
$\mu :=$ step size parameter
repeat
  $\mathbf{u}_{\mathrm{b}_{k+1}} := \mathbf{u}_{\mathrm{b}_k} + \mu(\alpha\hat{\mathbf{r}}_{pv} + (1-\alpha)\hat{\mathbf{R}}_{vv}\hat{\mathbf{u}}_{\mathrm{b}_k})$
  $\mathbf{u}_{\mathrm{b}_{k+1}} := \mathbf{u}_{\mathrm{b}_{k+1}}/\|\mathbf{u}_{\mathrm{b}_{k+1}}\|$
  $k := k+1$
until $(k = K)$ or alternatively $(\|\mathbf{u}_{\mathrm{b}_k} - \mathbf{u}_{\mathrm{b}_{k-1}}\|^2 < \varepsilon^2)$
Output: $\hat{\mathbf{u}} := \mathbf{u}_{\mathrm{b}_k}$

Interestingly, Eq. (A1) can be cast as an inhomogeneous eigenvalue problem $(1-\alpha)\hat{\mathbf{R}}_{vv}\mathbf{u}_{\mathrm{b}}+\alpha\hat{\mathbf{r}}_{pv}=\lambda\mathbf{u}_{\mathrm{b}}$, which is addressed in Ref. 36. This issue is beyond the scope of the current contribution.

[1]D. Levin, E. A. P. Habets, and S. Gannot, "On the angular error of intensity vector based direction of arrival estimation in reverberant sound fields," J. Acoust. Soc. Am. **128**, 1800–1811 (2010).

[2]D. Levin, E. A. P. Habets, and S. Gannot, "Impact of source signal coloration on intensity vector based DOA estimation," in *Proceedings of the International Workshop on Acoustic Echo and Noise Control (IWAENC)*, Tel-Aviv, Israel (2010).

[3]H.-E. de Bree, P. Leussink, I. T. Korthorst, D. H. Jansen, D. T. Lammerink, and P. M. Elwenspoek, "The microflown, a novel device measuring acoustical flows," in *8th International Conference on Solid-State Sensors and Actuators, and Eurosensors IX* (1995), Vol. 1, pp. 536–539.

[4]H. F. Olson, "Gradient microphones," J. Acoust. Soc. Am. **17**, 192–198 (1946).

[5]G. Elko and A.-T. N. Pong, "A steerable and variable first-order differential microphone array," in *IEEE International Conference on Acoustics, Speech, and Signal Processing (ICASSP)* (1997), Vol. 1, pp. 223–226.

[6]G. Elko and A.-T. N. Pong, "A simple adaptive first-order differential microphone," in *IEEE Workshop on Applications of Signal Processing to Audio and Acoustics* (1995), pp. 169–172.

[7]R. Derkx and K. Janse, "Theoretical analysis of a first-order azimuth-steerable superdirective microphone array," IEEE Trans. Audio, Speech, Lang. Process. **17**, 150–162 (2009).

[8]B. A. Cray and A. H. Nuttall, "Directivity factors for linear arrays of velocity sensors," J. Acoust. Soc. Am. **110**, 324–331 (2001).

[9]G. L. D'Spain, J. C. Luby, G. R. Wilson, and R. A. Gramann, "Vector sensors and vector sensor line arrays: Comments on optimal array gain and detection," J. Acoust. Soc. Am. **120**, 171–185 (2006).

[10]A. Nehorai and E. Paldi, "Acoustic vector-sensor array processing," IEEE Trans. Signal Process. **42**, 2481–2491 (1994).

[11]P. Tichavsky, K. Wong, and M. Zoltowski, "Near-field/far-field azimuth and elevation angle estimation using a single vector hydrophone," IEEE Trans. Signal Process. **49**, 2498–2510 (2001).

[12]P. Tam and K. Wong, "Cramér-Rao bounds for direction finding by an acoustic vector sensor under nonideal gain-phase responses, noncollocation, or nonorthogonal orientation," IEEE Sens. J. **9**, 969–982 (2009).

[13]D. P. Jarrett, E. A. P. Habets, and P. A. Naylor, "3D source localization in the spherical harmonic domain using a pseudointensity vector," in *European Signal Processing Conference (EUSIPCO)*, Aalborg, Denmark (2010).

[14]D. P. Jarrett, E. A. P. Habets, and P. A. Naylor, "Eigenbeam-based acoustic source tracking in noisy reverberant environments," in *Conference Record of the 44th Asilomar Conference on Signals, Systems and Computers (ASILO-MAR)*, Pacific Grove, CA (2010), pp. 576–580.

[15]K. Wong and H. Chu, "Beam patterns of an underwater acoustic vector hydrophone located away from any reflecting boundary," IEEE J. Ocean. Eng. **27**, 628–637 (2002).

[16]H. Cox, "Super-directivity revisited," in *Proceedings of the 21st IEEE Instrumentation and Measurement Technology Conference, IMTC 04* (2004), Vol. 2, pp. 877–880.

[17]Y. Wu, K. Wong, and S.-K. Lau, "The acoustic vector-sensor's near-field array-manifold," IEEE Trans. Signal Process. **58**, 3946–3951 (2010).

[18]D. Lubman, "Antifade sonar employs acoustic field diversity to recover signals from multipath fading," AIP Conf. Proc. **368**, 335–344 (1996).

[19]A. Abdi and H. Guo, "A new compact multichannel receiver for underwater wireless communication networks," IEEE Trans. Wireless Commun. **8**, 3326–3329 (2009).

[20]D. Levin, E. A. P. Habets, and S. Gannot, "Direction-of-arrival estimation using acoustic vector sensors in the presence of noise," in *IEEE International Conference on Acoustics Speech and Signal Processing (ICASSP)* (2011).

[21]J. DiBiase, H. Silverman, and M. Brandstein, "Robust localization in reverberant rooms," in *Microphone Arrays: Signal Processing Techniques and Applications*, edited by M. Branstein and D. Ward (Springer, New York, 2001), Chap. 8, pp. 157–180.

[22]S. Davies, "Bearing accuracies for arctan processing of crossed dipole arrays," in *Proceedings of Oceans'87* (1987), Vol. 1, pp. 351–356.

[23]F. Jacobsen and T. Roisin, "The coherence of reverberant sound fields," J. Acoust. Soc. Am. **108**, 204–210 (2000).

[24]M. Hawkes and A. Nehorai, "Acoustic vector-sensor correlations in ambient noise," IEEE J. Ocean. Eng. **26**, 337–347 (2001).

[25]I. Cohen and B. Berdugo, "Noise estimation by minima controlled recursive averaging for robust speech enhancement," IEEE Signal Process. Lett. **9**, 12–15 (2002).

[26]R. Hendriks, R. Heusdens, and J. Jensen, "MMSE based noise psd tracking with low complexity," in *IEEE International Conference on Acoustics Speech and Signal Processing (ICASSP)* (2010), pp. 4266–4269.

[27]A. Nehorai and M. Hawkes, "Performance bounds for estimating vector systems," IEEE Trans. Signal Process. **48**, 1737–1749 (2000).

[28]D. Serre, *Matrices: Theory and Applications*, Graduate Texts in Mathematics, 2nd ed. (Springer, New York, 2010), Chap 3, p. 53.

[29]M. S. Bartlett, "An inverse matrix adjustment arising in discriminant analysis," Ann. Math. Stat. **22**, 107–111 (1951).

[30]It should be noted that an ambiguity of 180° remains as multiplication of an eigenvector by -1 also produces an eigenvector (or from a different perspective, a dipole possess symmetric geometry with a rear lobe mirroring the main lobe). In Ref. 10, the ambiguity was resolved by assuming that the DOA search is initially constrained to a known half-space. In Ref. 20, the authors have suggested use of $\hat{\mathbf{r}}_{pv}$ to indicate the correct half-space. This approach is natural as it maintains continuity, corresponding to the limiting solution: $\lim_{\epsilon\to 0^+}\hat{\mathbf{u}}_{\mathrm{MSRP}}(\epsilon)$.

[31]H. Cox, R. Zeskind, and M. Owen, "Robust adaptive beamforming," IEEE Trans. Acoust., Speech, Signal Process. **35**, 1365–1376 (1987).

[32]S. M. Kay, *Fundamentals of Statistical Signal Processing: Estimation Theory* (Prentice-Hall, Upper Saddle River, NJ, 1993), Vol. 1, Chap. 7.

[33]An alternative criterion would be minimum noise, i.e., the target function to be minimized is noise variance $\mathbf{w}^T\mathbf{C}_e\mathbf{w}$ in place of output power $\mathbf{w}^T\mathbf{C}\mathbf{w}$. The solution resulting from this formulation is known as the Capon beamformer or minimum variance distortionless response (MVDR) beamformer. In cases where the DOA is accurately known, as we have assumed, the MPDR and MVDR beamformers are identical.

[34]H. Cox, "Resolving power and sensitivity to mismatch of optimum array processors," J. Acoust. Soc. Am. **54**, 771–785 (1973).

[35]H. L. Van Trees, *Optimum Array Processing*, Detection, Estimation, and Modulation Theory Vol. 3 (Wiley, New York, 2002), Chap. 6, p. 444.

[36]R. M. Mattheij and G. Söderlind, "On inhomogeneous eigenvalue problems. I," Linear Algeb. Appl. **88–89**, 507–531 (1987).